Food Biophysics (2026) 21:107
https://doi.org/10.1007/s11483-026-10186-w

RESEARCH

Exploratory Assessment of Ionic Liquid-Based Molecularly Imprinted Polymers for Potential Acrylamide Binding from Coffee Beverage

Robinson Monsalve-Atencio[1,2] · José Contreras-Calderón[2] · Francisco J. Morales[3] · Marta Mesías[3] · Luis F. Giraldo[1]

Received: 30 March 2026 / Accepted: 7 July 2026

Abstract
Acrylamide (AA) is a heat-induced process contaminant of toxicological concern associated with potential health risks. Its selective removal from complex food matrices, such as coffee brew, while preserving quality, remains a major technological challenge. This study explored an ionic liquid-based molecularly imprinted solid-phase extraction (MISPE) process for potential AA binding, combining molecularly imprinted polymers (MIPs) synthesized from polymerizable ionic liquid monomers with a packed-bed format. The effect of MISPE on coffee quality was examined through pH, total dissolved solids, colorimetric parameters and browning index. Among the four synthesized materials based on 2-(dimethylammonium) ethyl methacrylate [H-DMAEMA] and 2-(trimethylammonium) ethyl acrylate, the MIP synthesized with [H-DMAEMA] acetate exhibited the highest affinity toward AA in aqueous solution (dynamic imprinting factor: 1.72) and well-defined adsorption–desorption behavior fitted to the Boltzmann model. When applied to coffee brew, the MISPE process preserved physicochemical related parameters, including pH, total dissolved solids, and color. However, AA levels remained unchanged, likely due to competitive interactions with abundant macromolecules such as melanoidins and polysaccharides. These findings demonstrate the feasibility of ionic liquid-based imprinting for AA recognition in aqueous systems and highlight the physicochemical complexity of coffee as a model matrix for optimizing selective extraction strategies.

Keywords Coffee · Acrylamide removal · Molecularly imprinted polymer · Ionic liquid · Solid-phase extraction

Introduction

In foods like coffee, acrylamide (AA), an amide of high toxicological relevance [1] forms during the intermediate stage of the Maillard reaction, mainly through the reaction of the free asparagine with reducing sugars at temperatures above 120 °C and low-moisture conditions [2]. The International Agency for Research on Cancer (IARC) classifies AA as "probably carcinogenic to humans" [3]. Consequently, the European Union has established benchmark levels to reduce AA in food, setting 400 $\mu g \cdot kg^{-1}$ for roasted coffee and 850 $\mu g \cdot kg^{-1}$ for soluble coffee [4].

In coffee beverages, AA concentrations have been reported to range between 1.7 and 79.3 $\mu g \cdot L^{-1}$ [5], leading to estimated exposures of 10–565 ng/kg body weight/day [6]. AA exhibits no safe threshold in its dose-response relationship [7], and even minimal exposure may initiate carcinogenic processes. Consequently, the European Food Safety Authority (EFSA) and the Joint FAO/WHO Expert Committee on Food Additives (JECFA) recommended a margin of exposure (MOE) approach instead of defining a tolerable daily intake [8]. Reported MOE values for coffee consumption alone range from 75 to 8378, indicating a potential health concern since values below 10,000 are considered critical [9].

Several preventive and mitigation strategies have been proposed to reduce AA levels in coffee. Biotechnological approaches include fermentation and enzymatic treatments,

✉ José Contreras-Calderón
jose.contrerasc@udea.edu.co

1 Polymer Research Laboratory (LIPOL), Chemistry Institute, Faculty of Exact and Natural Sciences, University of Antioquia, Calle 67 No. 53–108, Ciudad Universitaria, Medellín, Colombia

2 Food Biotechnology Research Group (BIOALI), Food Department, Faculty of Pharmaceutical and Food Sciences, University of Antioquia, Calle 67 No. 53-108, Ciudad Universitaria, Medellín, Colombia

3 Institute of Food Science, Technology and Nutrition (ICTAN), Spanish National Research Council (CSIC), Jose Antonio Nováis 6, Madrid 28040, Spain

Published online: 03 August 2026

whereas formulation strategies focus on careful selection of mature coffee beans, adjusting mass balances according to species, and shorter brewing times [10–12]. However, mitigating AA in coffee remains challenging due to technological limitations and potential negative effects on sensory properties [13], highlighting the need for selective removal strategies.

A promising strategy for selective separations is molecular imprinting technology, which enables the synthesis of molecularly imprinted polymers (MIPs) [14]. These biomimetic materials, often referred to as "plastic antibodies," are obtained by forming pre-polymerization complexes between a target molecule (template of guest) and a functional monomer (host) (Fig. 1a). The resulting complex is copolymerized with a crosslinker (Fig. 1b), and subsequent template removal generates binding sites that are spatially and chemically complementary to the template, conferring selective recognition capability (Fig. 1c) [15, 16].

MIPs based on conventional monomers may exhibit relatively low extraction driving forces for hydrophilic analytes such as AA. This reduces the selectivity of conventional MIPs. This limitation can be addressed by using polymerizable ionic liquid (IL) monomers that promote extraction dominated by electrostatic interactions, such as permanent dipole-ion interactions, representing a more advanced driving force for extraction [17]. ILs are synthetic salts that are liquid at room temperature or below 100 °C, composed of an organic cation and an organic or inorganic anion [18]. When functionalized with polymerizable groups, they can act as monomers to form polyionic liquids, whose incorporation into MIPs enhances both extraction performance and physicochemical stability compared to MIPs based on conventional monomers [19, 20].

Although MIPs have been successfully developed for AA recognition in analytical applications [15, 16, 21], no biocompatible system has yet been evaluated for coffee detoxification. Therefore, this study assessed the adsorption performance of IL-based MIPs using a packed bed solid-phase extraction (SPE) process as a model for the selective binding of AA from coffee beverages. This represents the first evaluation of an ionic-liquid molecularly imprinted solid-phase extraction (MISPE) process for the removal of AA from a real coffee beverage.

Materials and Methods

Reagents and Materials

The medium-roasted, ground coffee sample, and the No. 2 paper filter bags were obtained from the local market in Medellín, Colombia. [$^{13}C_3$]-acrylamide (99% isotopic purity) was obtained from Cambridge Isotope Labs (Andover, MA). Acrylamide (AA purity≥99%) was purchased from Sigma-Aldrich (Germany). Methanol and ethanol (≥99.9%) were purchased from Honeywell (USA). Formic acid (98%), potassium hexacyanoferrate (II) 3-hydrate (Carrez I, 98%) and zinc acetate 2-hydrate (Carrez II, 99%) were obtained from Panreac (Barcelona, Spain). Empty LiChrolut® RP-18 polypropylene cartridges (6 mL), with frits used for MISPE of the coffee beverage, were purchased from Merck (Darmstadt, Germany). Oasis-HLB reverse phase cartridges (30 mg, 1 mL) were obtained from Waters (Milford, MA). Cellulose syringe filter units (0.22 and 0.45 µm) were obtained from Análisis Vínicos (Tomelloso, Spain). Ultrapure water (Type I) was obtained from the Barnstead™ Smart2Pure™ water purification equipment, Thermo Fisher Scientific™ (Sweden).

Preparation of Coffee Beverage

The coffee beverage was prepared using the Chemex method. A No. 2 paper filter was placed inside the device and moistened with water at 93 °C, which was then discarded. Roasted and ground coffee (22.5 g) was then added to the filter, and 120 mL of hot tap water (93 °C) was poured

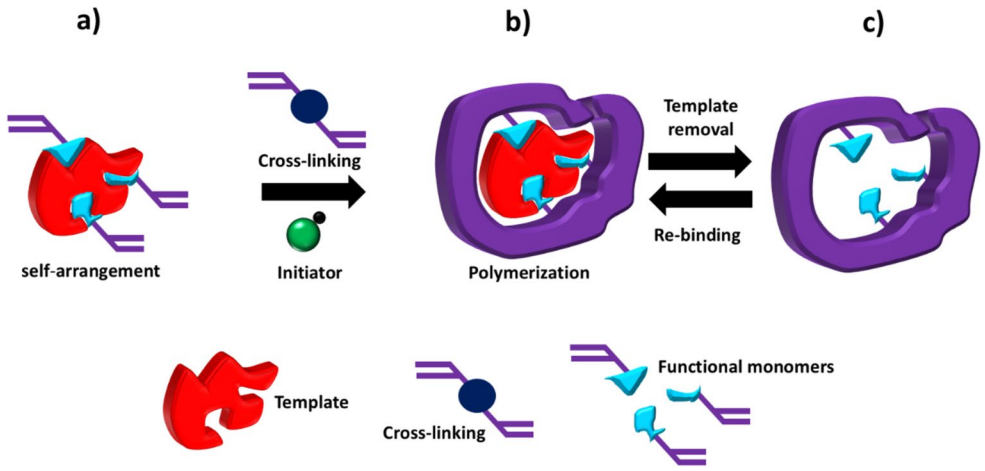

Fig. 1 Schematic representation of the molecular imprinting process

in three cycles over 3 min. The resulting coffee beverage was collected in airtight containers and cooled to 25 °C, which was the temperature used for the subsequent MISPE experiments [22, 23].

MISPE Process

In previous work [16], molecularly imprinted (MIPs) and non-imprinted polymers (NIPs) were synthesized and characterized using the conventional monomer DMAEMA and four ionic liquid (IL)-derived monomers: 2-(trimethylammonium) ethyl acrylate chloride [TMAEA][Cl] (Fig. 2a), 2-(trimethylammonium) ethyl methacrylate iodide [TMAEMA][I] (Fig. 2b), 2-(dimethylammonium) ethyl methacrylate acetate [H-DMAEMA][Ace] (Fig. 2c) and 2-(dimethylammonium) ethyl methacrylate acrylate [H-DMAEMA][Acr] (Fig. 2d). The structure of the IL monomers was characterized using Attenuated Total Reflectance Fourier Transform Infrared Spectroscopy (UATR/FTIR) and Proton Nuclear Magnetic Resonance (^{1}H NMR), while the morphology and structure of the MIPs and NIPs were characterized using Scanning Electron Microscopy (SEM) and UATR/FTIR (Fig. S1–15). These characterization analyses were conducted in our laboratory, and a highly detailed discussion of them was presented in an article previously published by our research group [16]. The porosity and specific surface area of the polymers were determined by nitrogen adsorption-desorption at 77 K using a Micromeritics ASAP 2020 Plus instrument (Micromeritics, USA). First, the samples were degassed under vacuum at 80 °C/4 h and then at 120 °C/2 h before measurement. The specific surface area and pore size distribution were calculated using the Brunauer-Emmett-Teller (BET) and Barrett-Joyner-Halenda (BJH) methods, respectively [24].

The MIPs were synthesized using conventional free-radical chain polymerization. It consists of three stages: a slow initial stage, followed by a propagation stage and a termination stage. The goal is to achieve rapid polymerization so that the sites imprinted with the template molecule can be established. The polymerization conditions were designed to preserve the template–monomer interactions during network formation, thereby enabling the generation of selective recognition sites complementary to the template molecule. To prepare the MIP, a monomer-template prepolymer complex was first obtained by stirring the functional monomer with the dummy molecule propanamide at 30 °C for 4 h in acetonitrile. During this pre-assembly stage, functional monomers such as [H-DMAEMA][Ace] can form ion-dipole interactions via their -NH_3^+ or COO^- groups with the amide group of the template (Fig. 3**)**. Once the MIP is obtained, these interactions will promote the formation of molecular memory and re-binding through chemical recognition. Subsequently, the radical initiator 1,1-azobis(cyclohexanecarbonitrile) (ABCN) was added under stirring and reflux at 80 °C for 1 h; after 23 h at 75 °C, the polymer was obtained via conventional free-radical precipitation polymerization. Finally, the polymer was washed, and the template molecule was removed, leaving behind molecularly imprinted cavities that are complementary to the AA in size, shape, and chemical functionality. The NIPs were obtained using the same methodology but without the addition of the template molecule. Dummy MIPs, together with their corresponding NIPs, were first evaluated in aqueous AA solutions through molecularly imprinted solid-phase extraction (MISPE). The MIP showing the best adsorption performance was then applied to the coffee beverage.

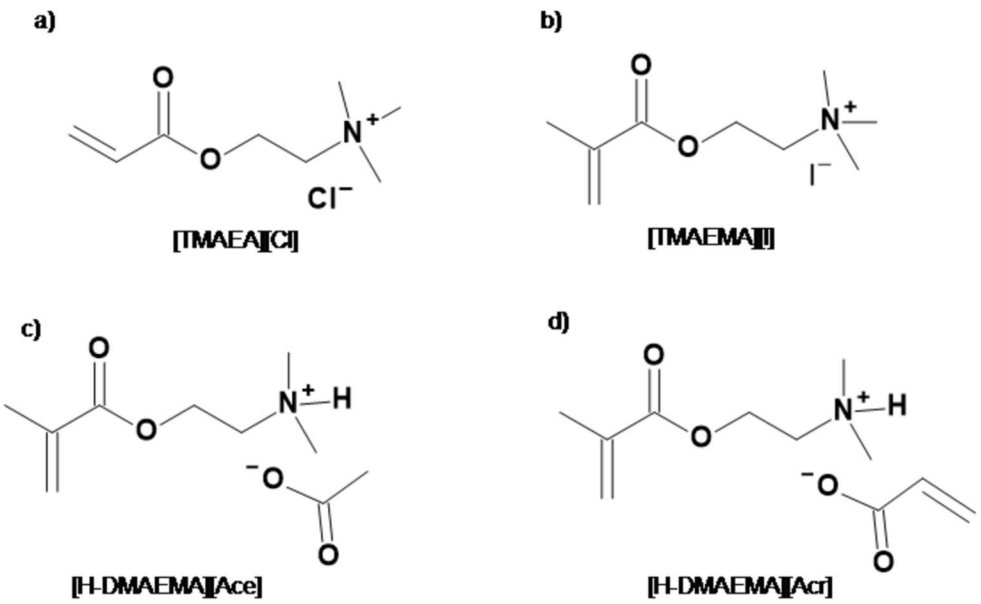

Fig. 2 Structure of (**a**) 2-(trimethylammonium) ethyl acrylate chloride [TMAEA][Cl], (**b**) 2-(trimethylammonium) ethyl methacrylate iodide [TMAEMA][I], (**c**) 2-(dimethylammonium) ethyl methacrylate acetate [H-DMAEMA][Ace] and (**d**) 2-(dimethylammonium) ethyl methacrylate acrylate [H-DMAEMA][Acr]

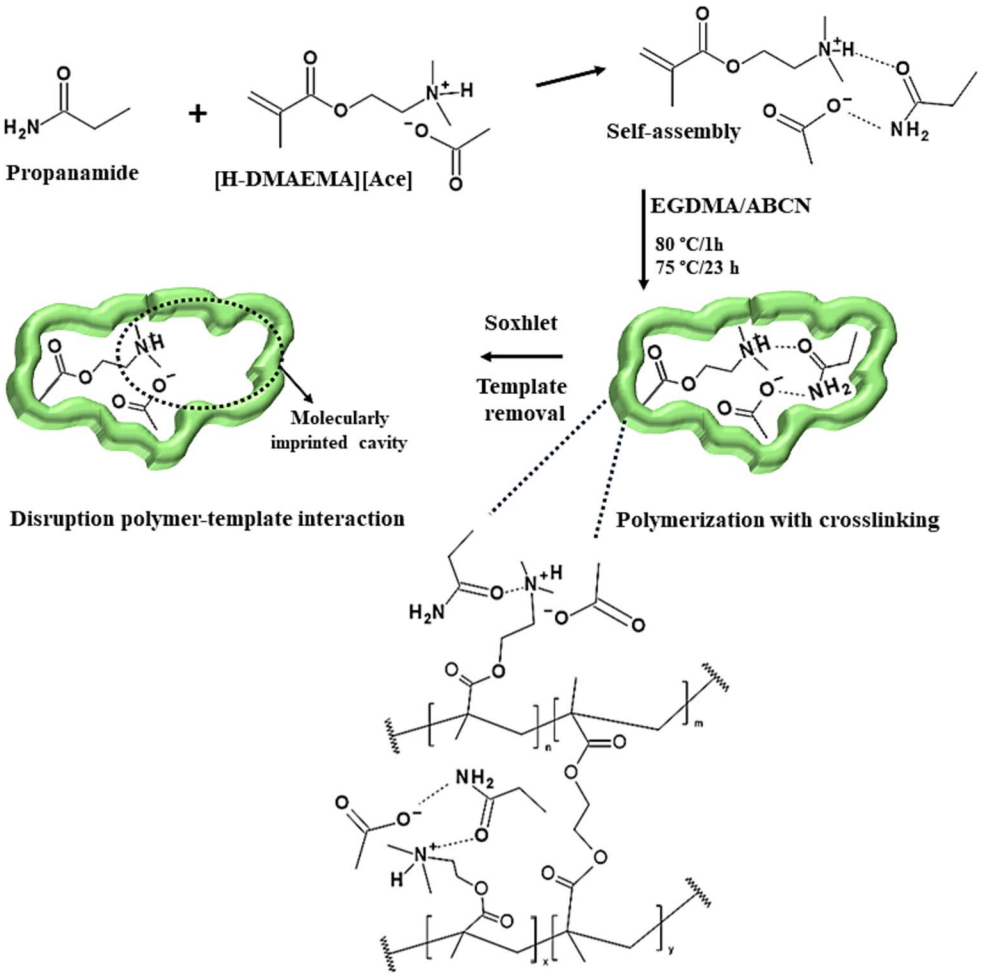

Fig. 3 Sketch of molecularly imprinted binding site formation process for selective AA recognition using the monomers [H-DMAEMA][Ace] and EGDMA

The extraction performance of the MIP was evaluated for both aqueous AA solution and coffee beverage. Approximately 150 mg of polymer were packed between two frits in an empty 6 mL SPE cartridge. The amount of polymer was selected so that it had the overscaled potential to retain AA according to the amount of analyte in the total sample volume and the adsorption capacity reported in a previous study [16]. The cartridge was activated by passing 1 mL of ethanol followed by 1 mL of distilled water at a flow rate of 1 mL·min^{-1}. Subsequently, the pure AA solution (at a concentration that is within the range commonly found in coffee beverages, 48.5 µg·L^{-1} [5] or coffee beverage was loaded at a flow rate of 0.5 mL·min^{-1}. The first 1.5 mL of eluted was discarded, and 1.5 mL fractions were collected up to 9 mL for AA solution or 75 mL for coffee beverage containing 63.8 ± 3.2 µg·L^{-1} of AA and 5.03 ± 0.06% tota dissolved solids (TDS). After elution, the cartridge was rinsed with 6 mL of water at 55 °C at 1 mL·min^{-1}.

Experimental data for AA concentration as a function of eluted volume were fitted using the Boltzmann model (Eq. 1) using OriginPro 8.0® software (OriginLab Corporation, Northampton, MA, USA).

$$\frac{C}{C_0} = A_2 + \frac{A_1 - A_2}{1 + exp^{\frac{V - V_0}{dV}}} \quad (1)$$

where C and C_0 represent the analyte concentrations in the eluate and feed, respectively. V is the percolation volume, e is Euler's number, and A_1, A_2, V_0, and dV are regression parameters.

From the fitted parameters, the performance of the MISPE process was estimated through several metrics: retention volume (V_R, mL, Eq. 2) [25, 26], hold-up volume (V_M, mL, Eq. 3) [27, 28], number of theoretical plates (N, Eq. 4, estimated based on V_B, Eq. 5) [29], retention factor (K, Eq. 6) [29, 30], efficiency index V_R/V_M [28], breakthrough capacity (Q_B, mL, Eq. 7) [29], bed capacity or dynamic capacity (Q_{dyn}, µg·g^{-1}, Eq. 8), and dynamic imprint factor (IF_{dyn}, Eq. 9) [31].

$$V_R = V_0 \quad (2)$$

$$V_M = V_0 + (dV) * ln\left(99 - 100 * \frac{A_1}{A_2}\right) \quad (3)$$

$$N = \frac{4V_R^2}{(V_B - V_R)^2} \quad (4)$$

Where V_B:

$$V_B = V_0 + (dV) * ln\lfloor \frac{100}{99}\left(1 - \frac{A_1}{A_2}\right) - 1\rfloor \quad (5)$$

$$K = \frac{V_M}{V_R} - 1 \quad (6)$$

$$Q_B = V_0 + (dV) * ln?\frac{100}{95}\left(1 - \frac{A_1}{A_2}\right) - 1? \quad (7)$$

$$Q_{dyn} = \frac{V_M * [Analite]_{in} - \int_0^{V_M}[Analite]_{out}\, dV}{m} - 1 \quad (8)$$

$$IF_{dyn} = \frac{Q_{dyn\,MIP}}{Q_{dyn\,NIP}} \quad (9)$$

Characterizations of Coffee Beverages from Roasted and Ground Coffee

Determination of AA by LC-ESI-MS-MS

AA concentration in the initial and eluted coffee beverages was determined following the methodology described by Mesías & Morales (2016) with slight modifications. 15.96 µL of [$^{13}C_3$]-acrylamide internal standard solution (5 µg·mL^{-1}) was added to 1.5 mL of sample. Then, 39.9 µL of Carrez I solution (15% m/v potassium hexacyanoferrate (II) 3-hydrate) and 39.9 µL of Carrez II solution (30% m/v zinc acetate 2-hydrate) were added. The mixture was vortexed for 5 s and centrifuged at 4 °C and 9000 g for 5 min. Supernatants were filtered sequentially through 0.45 and 0.22 µm cellulose filters, and 1 mL of filtrate was purified using Oasis-HLB cartridges (Waters Corp., Milford, MA), conditioned with 1 mL of methanol followed by 1 mL of distilled water at a flow rate of 2 mL·min^{-1}. The first few drops were discarded, and the remaining liquid was collected in an amber vial for LC-MS analysis [32].

AA quantification was performed using an Agilent 1200 liquid chromatograph coupled to an Agilent Triple Quadrupole MS detector (Agilent Technologies, Palo Alto, CA, USA). The sample (10 µL) was separated on an Inertsil ODS-3 column (250×4.6 mm, 5 µm; GL Sciences Inc., Tokyo, Japan) at 30 °C, using 0.2% (v/v) formic acid in water as the mobile phase at a flow rate of 0.4 mL·min^{-1} under isocratic elution. Electrospray ionization in positive mode was used, with AA eluting at 6.1 min and the needle set to 1.0 kV. The source temperature was 350 °C, and nitrogen was used as the nebulizer gas (12.0 L·min−1). The signal at m/z 72 - m/z 55 was isolated for AA and m/z 75- m/z 58 for [13C3]-acrylamide. For the transitions m/z 72>m/z 55 and m/z 75>m/z 58, fragmentation was set at a voltage of 76 V and collision energy of 8 V, and the masses were recorded using multiple reaction monitoring (MRM). For quantification, signals at m/z 75 and 78 were used, while signals at m/z 58 and 55 were used for qualification. AA was quantified using standard solutions (1–100 µg·L^{-1}) spiked with 50 µg·L^{-1} of [13C3]-acrylamide. Comparison of peak area ratios for the transitions m/z 72>55 and m/z 75>58 between sample extracts and standards confirmed peak identity. Results were expressed as µg·L−1 of beverage.

Total Dissolved Solids (TDS) and pH

Total dissolved solids (TDS) were estimated by measuring Brix degrees using the PAL-BX/RI digital refractometer (Atago®, Japan) and applying Eq. (10), which relates TDS concentration to Brix degrees [33, 34].

$$TDS = 0.87 *^{\circ}\ Brix \quad (10)$$

The pH of the coffee beverage was measured at room temperature using a pH meter HI 99,165 (HANNA, Colombia).

Non-Enzymatic Browning and Colorimetric Parameters

Non-enzymatic browning was measured in samples diluted 30-fold with distilled water, following the protocols of Gómez-Narváez et al. [35] and Nguyen et al. [36]. Optical density was recorded at 420 nm against the blank (distilled water) using a Mapada® UV-1200 UV-vis spectrophotometer.

Colorimetric analysis of coffee beverages was performed using a CR-20 colorimeter (Konica Minolta, INC., Japan). Color parameters were obtained according to the CIELAB color space. Results were expressed as lightness (L*), chroma (C*), hue angle (h), and color difference (ΔE). L*, C*, and h values were obtained directly from the spectrophotometer, while ΔE was calculated using Eq. 11. Measurements were referenced to the D65 daylight illuminant and a standard observer with a visual angle of 10°.

Statistical Analysis

The effect of MISPE treatment on the physicochemical and physical properties of the coffee beverage was evaluated using a completely randomized design. Differences between treatments were assessed by analysis of variance (ANOVA), followed by multiple range comparison tests, using Fisher's least significant (LSD) test at a 95% confidence level. Correlations among variables were examined using Pearson's

test, and data structure was explored through principal component analysis (PCA), retaining components with eigenvalues > 1. Analyses were performed with Statgraphics Centurion® 19 (version 19.1.2, 64 bit, 2020).

$$\triangle E : [(L^* - L^*_{ref})^2 + (a^* - a^*ref)^2 + (b^* - b^*_{ref})2]^{1/2} \quad (11)$$

Results and Discussion

Adsorption Efficiency of [H-DMAEMA][Ace]-Based MIPs for Acrylamide in SPE Systems

Aqueous Solution of Acrylamide

Polymers prepared from [TMAEMA][I] could not be tested in the SPE system, as they caused cartridge clogging that entirely obstructed solution flow, likely due to tighter packing associated with their finer particle size [16]. The adsorption behavior of AA from aqueous solution on the surface of the corresponding MIPs and NIPs packed in MISPE cartridges is shown in Fig. 4. Among the tested materials, the [H-DMAEMA][Ace]-based MIP (Fig. 4**a**) exhibited the best performance, reaching up to 83% A removal and showing the lowest normalized concentrations in the initial effluent fractions. After 3 mL of eluate, adsorption gradually decreased until equilibrium was reached. These results demonstrate that MIPs embedded in fixed-beds SPE can effectively retain AA in aqueous solution, consistent with previous findings obtained for dispersed MIP systems in acetonitrile [16].

The main adsorption parameters derived from Boltzmann fitting are summarized in Table 1. The breakthrough capacity (Q_B) represents the mobile phase volume corresponding to 5% of the maximum analyte concentration in the effluent, reflecting a combination of mass transfer kinetics, static binding capacity, and dispersion, thus indicating the actual working capacity of the polymer [29]. The dynamic imprinting factor (IF_{dyn}) reflects the number of instances in which MIP demonstrated superior adsorption capacity relative to the NIP; higher IF_{dyn} values indicate greater efficiency and selectivity of the MIP over its non-imprinted counterpart [37]. A V_R/V_M ratio closer to 1 indicates that the hold-up volume (V_M) is rapidly reached once the retention volume (V_R) is attained, resulting in more efficient adsorption. Similarly, process efficiency is related to the number of theoretical plates (N), with higher N values indicating greater efficiency [30]. Conversely, a lower retention factor (K) is associated with better SPE performance, as it reflects a lower V_M relative to V_R, suggesting faster polymer saturation after V_R, and improved mass-transfer dynamics [38].

Among all tested polymers, M@[H-DMAEMA][Ace] exhibited the highest AA extraction performance across

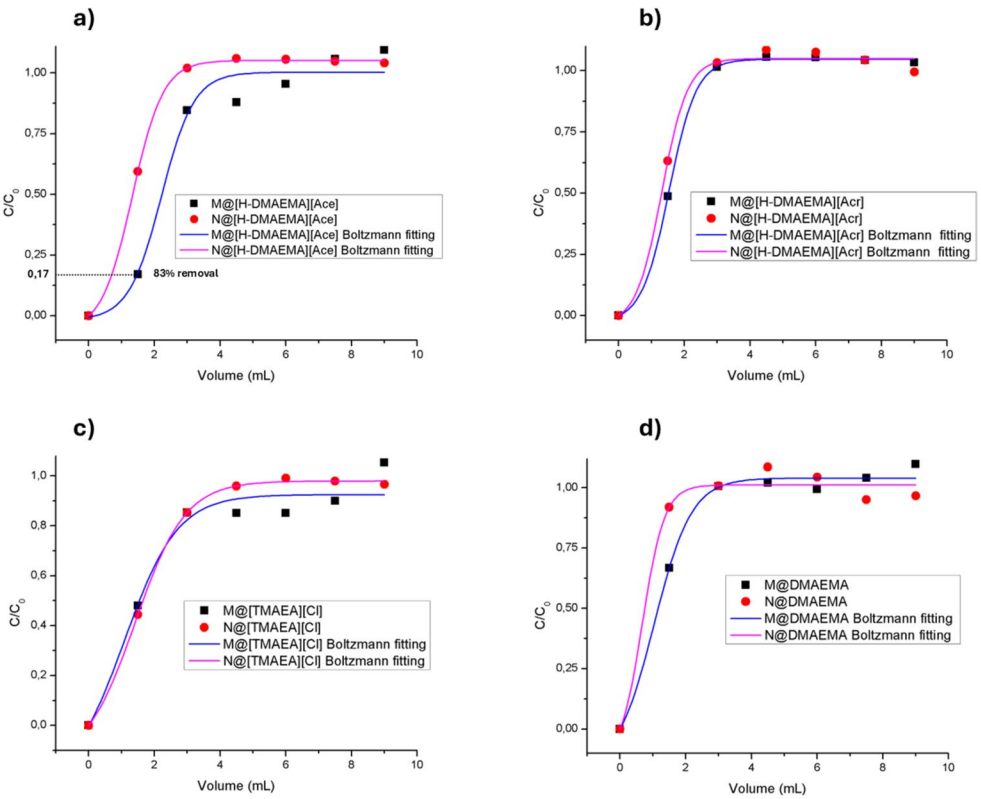

Fig. 4 Breakthrough curves fitted using the Boltzmann model for AA adsorption in normalized pure solution in MIPs (black squares) and NIPs (red circles) based on (**a**) [H-DMAEMA][Ace], (**b**) [H-DMAEMA][Acr], (**c**) [TMAEA][Cl] and (**d**) DMAEMA

Table 1 Parameters used to fit the Boltzmann model to AA adsorption breakthrough data in aqueous solution

	[H-DMAEMA][Ace]		[H-DMAEMA][Acr]		[TMAEA][Cl]		DMAEMA	
	MIP	NIP	MIP	NIP	MIP	NIP	MIP	NIP
Q_B (mL)	0.90	0.31	0.48	0.37	0.19	0.25	0.18	0.13
Q_{dyn} (ng·g^{-1})	734.0	427.2	484.7	409.2	605.8	588.1	395.4	261.9
IF_{dyn}	1.72	-	1.18	-	1.03	-	1.51	-
V_R/V_M	0.49	0.38	0.44	0.42	0.22	0.28	0.28	0.30
N	6.09	4.52	4.88	4.71	4.34	4.33	4.33	4.35
K	1.03	1.64	1.25	1.37	3.56	2.55	2.59	2.33
R^2-adj	0.95	1.00	1.00	0.99	0.93	1.00	0.99	0.97

all evaluated parameters (Table 1). This outcome suggests advantages in hydrogen bond basicity, polarity (dielectric constant (ε), donor number (DN), and acceptor number (AN)), and enhanced acid-base interactions with AA [16]. The Kamlet-Taft basicity scale parameter, β, suggests that hydrogen-bonding ability (HBA) serves as a measure of proton acceptance or electron pair donation. Other studies have also found that the extraction driving force was influenced by the β-hydrogen-bonding basicity of the anions in these ILs, with the $[Ace]^-$ anion exhibiting higher β-basicity than the $[Cl]^-$ anion. This relatively strong basicity induces high polarity in the IL due to its highly localized charge. The polarity of the IL monomers may influence the AA adsorption capacity of the polymers under study. One way to express polarity is through the dielectric constant ε, DN, and AN, where it has been reported that protic ILs exhibit higher polarity than aprotic ones, a finding consistent with the comparison of the Q_{dyn} and IF_{dyn} values of the $[Ace]^-$ anion relative to the $[Cl]^-$ anion [16].

Polymers derived from monomers such as M@[H-DMAEMA][Ace] may therefore be more suitable for applications involving direct contact with consumer products, such as coffee beverages. Notably, no cytotoxicity has been reported for monomers based on DMAEMA [39]. In contrast to conventional IL monomers derived from imidazole, which are frequently associated with toxicity, IL monomers synthesized from DMAEMA and acetic acid, a compound commonly used as food additive [40], offer a more biocompatible alternative.

Surface Properties of MIPs

All isotherms exhibited a convex shape throughout the entire range of relative pressure (P/P_0) and corresponded to Type III isotherms according to the IUPAC classification (Figs. S16–19). This indicates that the interactions between the adsorbed molecules are stronger than those between the adsorbate and the surface. The rebinding of the analyte is governed by the molecular imprinting effect rather than by the porosity of the system. The [TMAEA][Cl]-based MIP exhibited higher nitrogen adsorption at low relative pressures, showing the highest BET surface area (14.1 m²/g), followed by DMAEMA-based MIP (12.3 m²/g), [H-DMAEMA][Acr]-based MIP (4.6 m²/g), and [H-DMAEMA][Ace] (2.0 m²/g) (Table S1). This trend correlates well with the morphologies observed by SEM (Fig. S10), where smaller polymer particles (e.g., MIP based on [TMAEA][Cl]) exhibited larger surface areas. Therefore, it is important to highlight that although the [H-DMAEMA][Ace]-based polymer had the smallest surface area (Table S1), it exhibited the highest adsorption performance (Table 1). This indicates that the performance is due to specific adsorption processes resulting from the molecularly imprinted cavities, rather than surface area, which is a valuable attribute of molecularly imprinted systems.

Coffee Beverage

The [H-DMAEMA][Ace]-based MIP, identified as the most effective in aqueous AA solutions, was subsequently evaluated in a fixed-bed SPE system using coffee beverage. As shown in Fig. 5, the AA concentration in the coffee beverage effluent remained relatively stable up to a final volume of 75 mL, with values ranging from 56 ± 2.8 to 71.2 ± 3.6 μg·L^{-1}. These concentrations are consistent with those previously reported for coffee beverages [5, 41]. The absence of a decreasing trend indicates that, under these conditions, the MISPE process did not achieve detectable AA removal from the coffee matrix.

In a previous study, an effective AA removal process was achieved using a MIP based on [H-DMAEMA][Ace], synthesized with acetonitrile as the porogenic solvent [16]. However, the extraction was performed in agitation and dispersion systems, rather than in a cartridge-packaged format employed in the present study. Acetonitrile was used as the extraction solvent, a condition that does not simulate the real medium in which AA is typically found, namely, an aqueous coffee beverage. Acetonitrile is an aprotic solvent, incapable of forming hydrogen bonds because it lacks hydrogen atoms bonded to electronegative atoms such as oxygen or nitrogen. This property allows precise control over the specific interactions between the functional monomer and the template molecule,

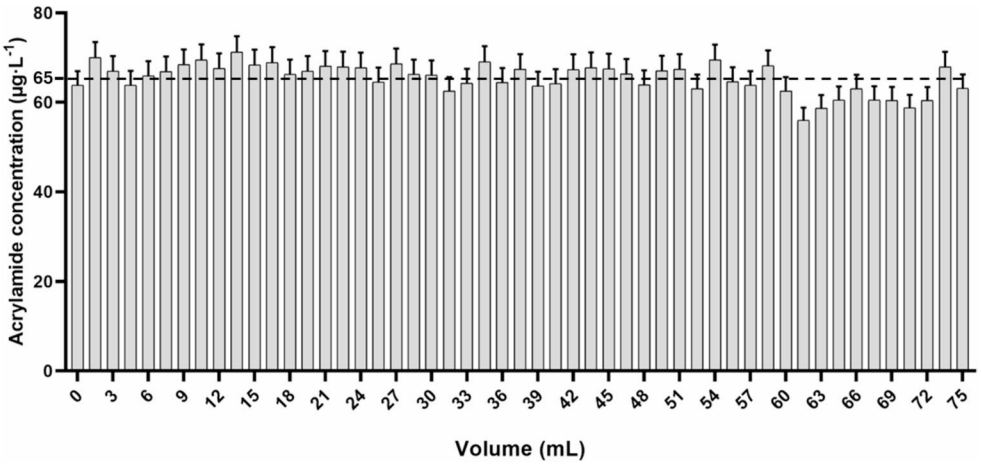

Fig. 5 Concentration of AA in coffee beverage effluent from roasted and ground coffee during the MISPE process using M@[H-DMAEMA][Ace]

as acetonitrile does not interfere with hydrogen bonding or electrostatic forces. Thus, it facilitates the re-binding process [42], as previously observed [16]. However, MIPs generally exhibit reduced adsorption capacity for the target molecule when tested in solvents different from those used during polymer synthesis, a phenomenon attributed to the so-called molecular memory effect, which was confirmed in this study. Likewise, when hydrophilic analytes are extracted using solvents more polar than those employed during MIP synthesis, re-binding efficiency tends to decrease significantly [42, 43]. This trend was also evident in our experiments, as the coffee beverage represents an aqueous medium. Compared with acetonitrile, water exhibits markedly higher values of dielectric constant (ε), dispersion forces (δ_d), polar forces (δ_p), hydrogen-bonding forces (δ_H), and solvatochromic polarity (E_T), making it a substantially more polar solvent [42]. Therefore, water was able to compete with the MIP for AA binding sites, thereby impeding the detoxification of the coffee beverage.

Coffee is a highly complex matrix consisting mainly of water and high-molecular-weight polymers such as melanoidins and polysaccharides (e.g. galactomannans and arabinogalactans), as well as lipids, minerals, organic acids, phenolic acids (notably chlorogenic acids), and nitrogenous compounds such as caffeine and trigonelline [44]. Several of these components may interact with AA or with the MIP surface, interfering with the selective adsorption of AA. Moreover, coffee beverages contain not only neutral aprotic compounds but also acidic and conjugated ionic species derived from coffee solids, together with ions such as Na^+, $Mg^{2+,}$ and Ca^{2+} originating from the tap water used for preparation [44, 45]. Considering the charged surface of the MIP, these ionic species may compete for active adsorption sites via electrostatic interactions, thereby limiting AA adsorption, particularly considering its low concentration relative to other coffee constituents.

Melanoidins are polyfuncional high-molecular-weight polymers that can exhibit either positive or negative charges [46]. In fact, the polyanionic character of coffee melanoidins enables their isolation from the beverage using SPE materials [47]. Analogously, during the percolation process, a fraction of the melanoidins content in the coffee beverage may be adsorbed onto the molecularly imprinted ionic liquid polymer via electrostatic interactions between the charged adsorbent and adsorbate. Although this fraction may be small, the adsorbed melanoidins could form a superficial layer that acts as a physical barrier, thereby hindering AA adsorption. This effect is particularly relevant considering that AA is a small molecule (71.08 $g \cdot mol^{-1}$), present at very low concentrations in the coffee beverage (63.8 $\mu g \cdot L^{-1}$, Fig. 5), whereas melanoidins are high-molecular-weight polymers of 3 to 22 kDa [48] and may account for up to 23% (w/w) of he dry weight of coffee beverage [49]. This behavior supports the existence of a competitive matrix effect caused by other constituents of the coffee beverage (melanoidins, conjugated acids and salts, and various ions), many of which are present at higher concentrations and molecular sizes than AA.

Melanoidins, as functionalized polymers, can retain or trap various substances and can even form covalent bonds with a wide range of small molecules [46, 50, 51]. Melanoidins can be functionalized with ester (C = O), amine (N–H), and aromatic (C–N) groups [49], which can interact with AA. In addition to this steric effect, melanoidins can chemically interact with AA. Pastoriza et al. (2012) demonstrated that model coffee melanoidins can react with AA through Michael-type additions between nucleophilic amino groups and the α,β-unsaturated carbonyl of AA, forming stable adducts [52]. Such covalent or strong non-covalent associations may reduce the free AA available for adsorption by the MIP. Together with the high abundance and macromolecular size of melanoidins, these interactions likely explain the negligible extraction observed [52]. Furthermore, because the MIP is fixed in bed, it faces a competitive disadvantage compared with other polymers in the coffee beverage that are

dispersed under dynamic conditions, which may favor the adsorption of AA onto components other than MIP. Therefore, a potential improvement in the AA re-binding process on the MIP could be explored by dispersing and stirring the polymer in the coffee beverage due to a higher probability of collision and kinetic energy. To recover the polymer from the coffee beverage after adsorption, magnetic field extraction could be used, which could be carried out using a core (Fe_3O_4)-shell (MIP) format involving surface imprinting, another molecular imprinting strategy that improves mass transfer and adsorption-desorption efficiency for extraction and reusability [53].

Like melanoidins, polymeric compounds such as galactomannans and arabinogalactans may compete with AA for adsorption onto the MIP, as they contain -OH and -COOH groups capable of interacting with the MIP's functional groups. Furthermore, the functional groups present in galactomannans and arabinogalactans may facilitate AA adsorption via interactions with its amide group [21], resulting in its retention on their surface and thereby limiting the elimination of this contaminant in the coffee beverage. Additionally, coffee is a polyphasic beverage in which not only water-soluble components of roasted and ground coffee are extracted during preparation, but also a fraction of the lipids presents in the roasted product [44]. Consequently, it is possible that lipids in the coffee infusion similarly create a shielding effect on the molecularly imprinted surface, obstructing AA adsorption [54].

Effect of the MISPE Process on Some Physicochemical and Physical Properties of Coffee Beverage

pH and Total Dissolved Solids (TDS)

Figure 6a shows the evolution of pH values during the MISPE process. It was observed that pH increased significantly ($p < 0.05$) in the first fractions of the effluent volume. However, from 7.5 mL onwards, the effluent pH did not show significant differences compared to the coffee beverage prior to the MISPE process. These results suggest that, although the MISPE process temporarily affects the pH of the coffee beverage during the initial percolated volumes, the pH eventually stabilizes to a value similar to that of the original sample. The pH values obtained were within the range reported in the literature for coffee beverages [36, 55].

AA is a very weak base that, at pH values below 3.0, can be protonated and carry a positive charge in its structure [21]. This protonation could enhance its re-binding through electrostatic interactions during the MISPE process due to the ionic nature of the polymer (M@[H-DMAEMA][Ace]). However, under the pH conditions of coffee beverage effluent (Fig. 6a), AA is predominantly in its molecular (neutral) form, so no improvement in the adsorption would be expected as a result of the beverage's pH. Conversely, it has been reported that the adsorption mechanism of AA on other materials may still be influenced by pH. Although at pH values near 5.0 AA is neutral, the binding efficiency may increase because functional groups on the adsorbent, such as the $-NH_2$ groups, can acquire a positive charge and interact ionically with the carbonyl group (C = O) of AA [21]. Coffee beverages contain a variety of charged species, which may cause the polar AA molecule to interact preferentially with them, thereby limiting its adsorption in the MISPE system.

Similar to the pH behavior observed during the initial fractions of the effluent volume, the total dissolved solids (TDS) content decreased significantly ($p < 0.05$) in the first 9 mL of percolated extract (Fig. 6b). However, after 10.5 mL, no significant differences were observed compared to the untreated sample ($p > 0.05$). The initial decrease in TDS concentration suggests that portion of the solids present in coffee may contribute to the matrix effect that limits AA adsorption. Similar TDS values have been reported for coffee beverages in other studies [56].

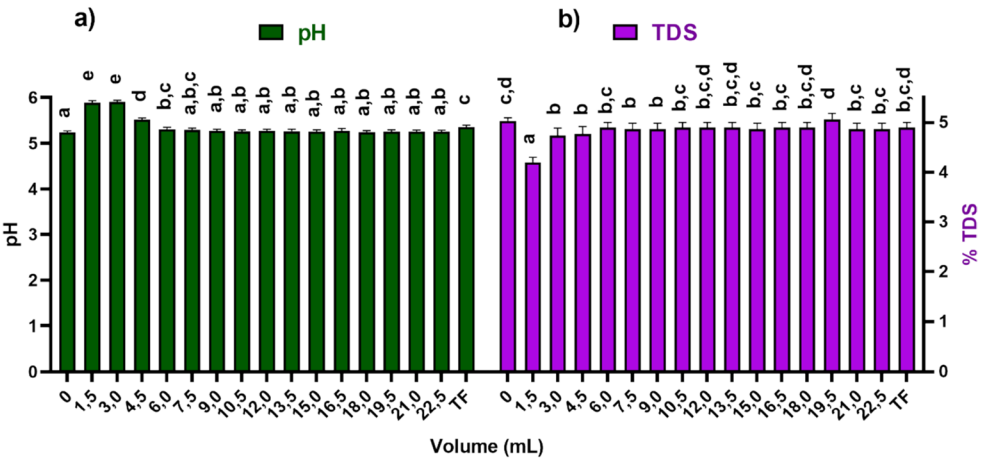

Fig. 6 Effect of the MISPE process on (**a**) pH and (**b**) total dissolved solids (TDS) in the coffee beverage effluent from roasted and ground coffee using M@[H-DMAEMA][Ace]. Means with different letters indicate significant differences ($p < 0.05$)

Colorimetric Parameters and Browning Index

Absorbance at 420 nm, which correlates with melanoidin concentration, enables the evaluation of caramelization and Maillard reactions progression, as this wavelength corresponds to the maximum absorption peak of these compounds [36]. Figure 7 shows the color parameters and browning index values, which are consistent with those reported in other studies [36, 57]. Although slight color differences were observed, ΔE values below 2 were obtained, indicating no visually perceptible changes and, therefore, no loss of visual quality [58, 59]. While the MISPE process did not significantly affect C* and *h* values across all total fractions (TF), L* values increased, and the browning index decreased during the first fractions of the coffee beverage volume ($p < 0.05$). These changes indicate that the coffee beverage extracts became lighter in color and contained fewer melanoidins during the first 4.5 and 6.0 mL, respectively. This suggests that the portion of the melanoidins in the coffee beverage were adsorbed onto the MIP surface until equilibrium was reached [46, 60]. Even the small amount of melanoidins adsorbed could be sufficient to block the active sites of the MIP for selective adsorption.

Pearson Correlation Analysis

Significant negative correlations were found between pH and both TDS content and the browning index (melanoidins, Abs 420 nm), while positive correlations were observed with L* and ΔE (Fig. 8). This result indicates that a decrease in TDS and melanoidin content leads to an increase in the pH of the coffee beverage, resulting in a lighter color and, although slightly, showing a greater overall color difference.

A significant positive correlation was also found between TDS and melanoidin content (Abs 420 nm), suggesting that decreases in TDS are accompanied by reductions in melanoidins. This finding agrees with previous reports, which indicate that melanoidins account for between 11 and 43% of the dry fraction of coffee [46, 61]. Similarly, other authors have also reported positive correlations between the browning index and TDS [36, 55]. Melanoidins are known to be brown-colored compounds that have a major influence on coffee color [62]. Therefore, lower TDS and melanoidin levels are associated with lighter coffees, which explains the strong negative correlation between L* and both TDS and melanoidins, as well as the strong positive correlation between the L* and ΔE.

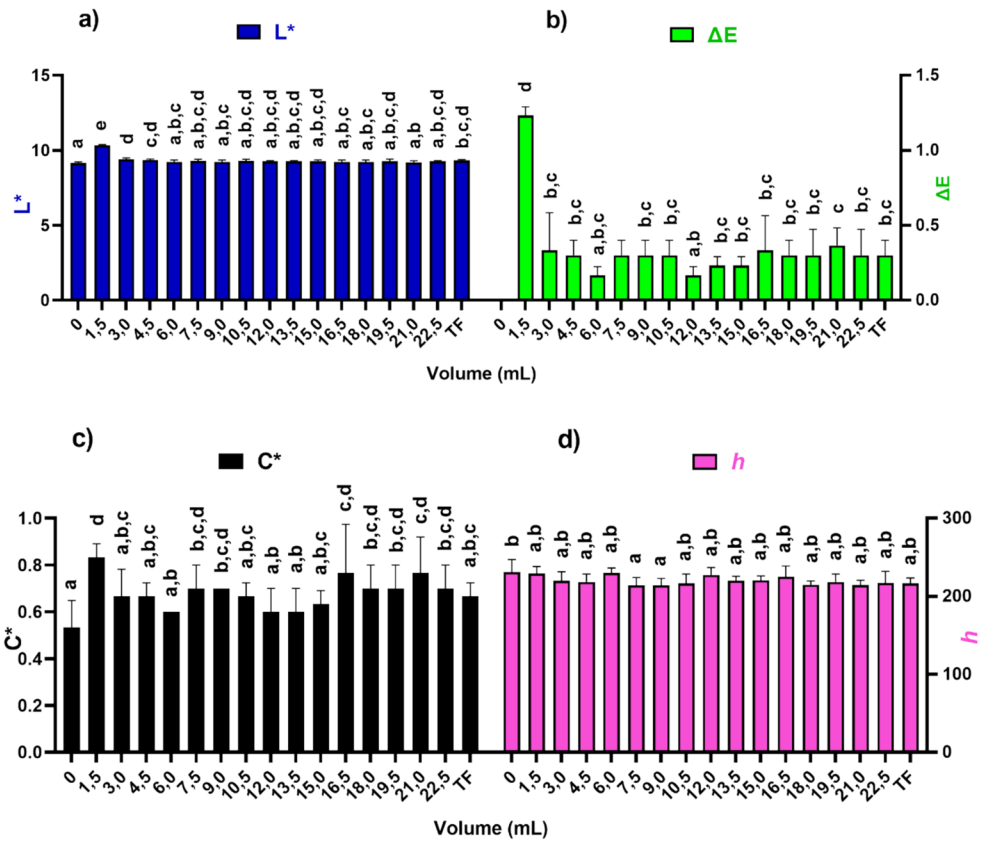

Fig. 7 Effect of the MISPE process on some color parameters: (**a**) lightness, L*; (**b**) color difference, ΔE; (**c**) chroma, C*; (**d**) hue, *h*, and (**e**) browning index of coffee beverage effluent. Means with different letters indicate significant differences ($p < 0.05$)

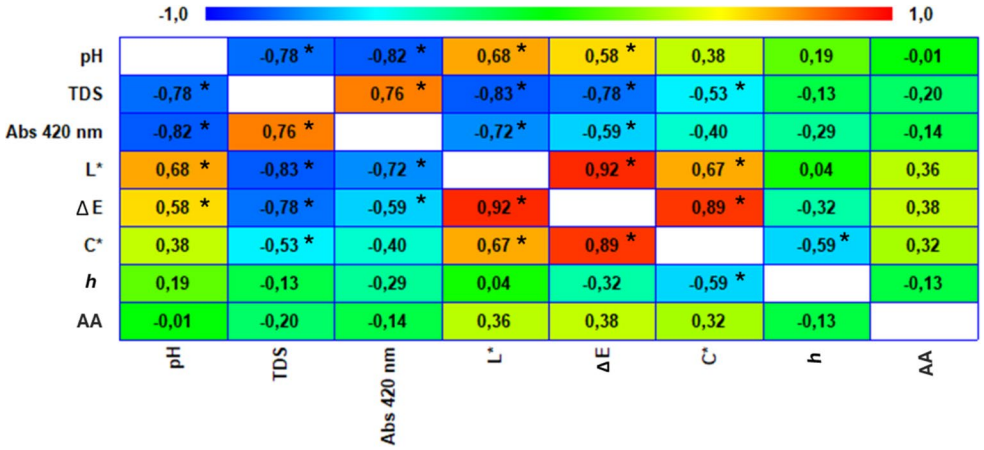

Fig. 8 Pearson correlation matrix between physicochemical properties and color during the MISPE process. Values marked with an asterisk (*) indicate significant correlations ($p<0.05$). TDS: % total dissolved solids, Abs 420 nm: browning index

Other studies have also reported negative correlations between brown compounds (melanoidins, Abs 420 nm) and the L* value [63]. Finally, variations in ΔE were positively related to slight changes in C*, further supporting the observed color dynamics.

Results reported by other authors also suggest a negative correlation between pH and total solids content [55]. Among the solids in coffee infusion are organic acids such as chlorogenic acids, which account for approximately about 16% (/m) [46] and can influence the pH of the beverage [64]. This could explain the inverse relationship between total solids and pH values, since a decrease in solids also implies a reduction in organic acid content, potentially leading to a decrease in pH. Similar results have been reported in the literature [65]. Likewise, the inverse relationship observed between pH and melanoidin content may be explained by the direct relationship between TDS and melanoidins: a decrease in melanoidins is associated with a reduction in TDS, which, in turn, is related to an increase in pH, as previously discussed. Other studies have also reported a negative correlation between pH the content of brown compounds (Abs 420 nm) [55], which could be attributed to the fact that various acids, such as chlorogenic and quinic acids, can bind ionically to melanoidins, thereby inversely affecting the pH of the infusion [66].

On the other hand, it showed a correlation only with the C* parameter and did not exhibit significant correlations with the other variables analyzed, as it did not undergo significant changes during the MIPSE process (Fig. 8). This behavior was similar to that of the AA content (Fig. 5) in the coffee beverage, which also did not show significant variations during the percolation process and, therefore, could not be statistically correlated with the characterization parameters studied. This is consistent with the findings of other authors, who reported no significant correlations between AA content and other variables such as pH, total solids, and browning index (melanoidins) [32].

Principal Component Analysis (PCA)

Two principal components were extracted, accounting for 79.49% of the total variance (Fig. 9). Principal component 1 (PC1), which explained 57.06% of the variance, showed positive loadings for L*, ΔE, pH, and C*, and was therefore mainly associated with color and pH. PC1 also presented negative loadings for TDS and Abs 420 nm, which are related with the melanoidin content. Principal component 2 (PC2) explained 22.43% of the variance and was negatively influenced by *h* and pH, while showing positive loadings for C*, Abs 420 nm, and, to a lesser extent, AA content, which did not correlate with any of the studied variables. The PCA pattern corroborated the Pearson correlation, highlighting the inverse relationship between TDS, and melanoidin content, with pH and L* values.

Although it was not possible to remove the AA, this study confirms that the MISPE process induced only transient changes in the composition of coffee beverages without altering their overall physicochemical balance. This stability supports the polymer's compatibility with beverage matrices and its potential for future optimization in dynamic extraction systems. Additionally, this study presents a clear scientific explanation for understanding the matrix effect on AA retention and lays the groundwork for further research in this field.

Conclusions

This study provides an exploratory assessment of ionic-liquid-based molecularly imprinted polymers for the potential binding of acrylamide (AA). While the [H-DMAEMA][Ace]-derived MIP demonstrated significant adsorption capacity in controlled aqueous solutions, its performance was severely constrained when applied to the complex coffee beverage matrix. The results indicated that selective

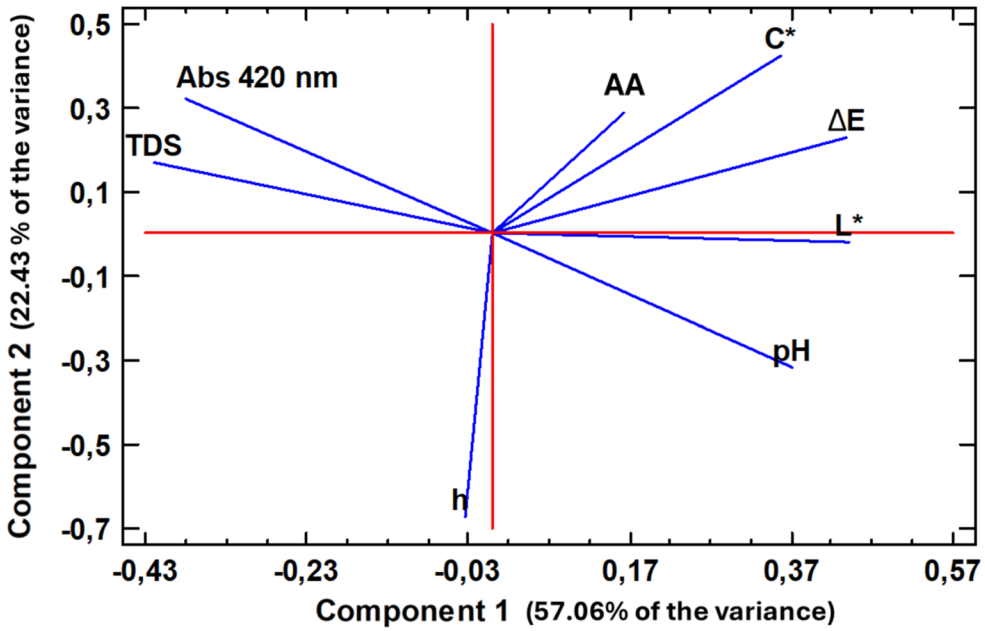

Fig. 9 Principal component analysis (PCA) of the coffee beverage effluent from roasted and ground coffee obtained during the MISPE using M@[H-DMAEMA][Ace] according to color parameters, physicochemical, and AA content

recognition was inhibited in the actual beverage. This technical limitation is attributed to competitive adsorption of abundant coffee constituents, such as melanoidins and polysaccharides, which likely block the polymer´s active sites or interact with AA molecules, preventing their capture. Despite the lack of analyte removal, the process preserved the physicochemical integrity of the beverage (pH, color, and solids content), suggesting the material´s basic compatibility with food matrices. To address these mass transfer limitations and site competition, future research should transition from static systems toward dispersion-based strategies combined with surface molecular imprinted for magnetic solid-phase extraction (MSPE). Such dynamic systems may enhance the collision probability between AA and the absorbent surface, potentially facilitating more efficient separation in chemically dense environments.

Supplementary Information The online version contains supplementary material available at https://doi.org/10.1007/s11483-026-10186-w.

Acknowledgements The authors would like to thank Ms. Manuela Gallego Villada and Ms. Yadiela Mosquera, Mr. Pablo Pacheco, Yuder Garcia Valencia, and Dr. Esneyder Ruiz for supporting this research.

Author contributions Robinson Monsalve-Atencio: Conceptualization, data curation, investigation, methodology, formal analysis, visualization, writing – original draft. José Contreras-Calderón: Conceptualization, data curation, investigation, methodology, formal analysis, visualization, funding acquisition, project administration, review and editing. Francisco J. Morales: Conceptualization, data curation, investigation, methodology, formal analysis, visualization, review and editing. Marta Mesías: Conceptualization, data curation, investigation, methodology, formal analysis, visualization, writing – review and editing. Luis F. Giraldo: Conceptualization, data curation, investigation, methodology, formal analysis, visualization, review and editing.

Funding Open Access funding provided by Colombia Consortium. This work was supported by the Universidad de Antioquia (UdeA), Committee for the Development of the Investigation (CODI) under Grant 2020–33944, and Doctoral scholarship for best graduate N.CA063; We thank the Sapiencia Post-secondary Education Agency of Medellín, National Postgraduate Fund - Extending Educational Frontiers Resolution number 6437 (July 29, 2020), grantee 1032259470.

Data Availability Data will be made available on request.

Declarations

Competing interests The authors declare no competing interests.

References

1. L.O. Rocha, J.C. Contreras-Calderón, R. Monsalve-Atencio et al., Coffee Components: Acrylamide, Mycotoxins, and Furan, in *Coffee and Human Health: Chemistry and Mechanisms of Action*, ed. by G. Grosso (Royal Society of Chemistry, 2025), pp. 298–323
2. V. Gökmen, *Acrylamide in food: Analysis, content and potential health effects* (Academic, New York, 2015)

3. IARC, Acrylamide. IARCmonographs on the evaluation of carcinogenic risks to humans. Some industrial chemicals. **60**, 389–434 (1994)
4. European Commission, COMMISSION REGULATION (EU) 2017/2158 of 20 November 2017 establishing mitigation measures and benchmark levels for the reduction of the presence of acrylamide in food. Official J. Eur. Union. **L304**, 24–44 (2017)
5. B. Basaran, Y.D. Özbek, (2025) Chap. 66 - Formation, level, reduction methods, and health risk assessment of acrylamide in coffee products. In: Preedy VR, Patel VB (eds) Coffee in Health and Disease Prevention (Second Edition). Academic Press, pp 743–751
6. A.P. Arisseto, E. Vicente, *Chap. 65 - Estimate of Acrylamide Intake from Coffee and Health Risk Assessment*, ed. by V.R.B.T.-C. Preedy in, H and DP (Academic, San Diego, 2015), pp. 575–584
7. J. O'Brien, A.G. Renwick, A. Constable et al., Approaches to the risk assessment of genotoxic carcinogens in food: A critical appraisal. Food Chem. Toxicol. **44**, 1613–1635 (2006). https://doi.org/10.1016/j.fct.2006.07.004
8. FAO/WHO, *World Health Organization* (Food and Agriculture Organization of the United Nations, Geneva; Rome, 2011)
9. EFSA, Scientific Opinion on acrylamide in food. EFSA J. **13**, 4104 (2015)
10. M. Anese, (2015) Furan and Other Furanic Compounds in Coffee: Occurrence, Mitigation Strategies, and Importance of Processing. In: Preedy V (ed) Processing and Impact on Active Components in Food. London, pp 541–547
11. M. Anese, Acrylamide in coffee and coffee substitutes, in *Acrylamide in food: Analysis, content and potential health effects*, ed. by V. Gökmen (Elsevier, 2016), pp. 181–195
12. G. Strocchi, P. Rubiolo, C. Cordero et al., Acrylamide in coffee: What is known and what still needs to be explored. A review. Food Chem. **393**, 133406 (2022). https://doi.org/10.1016/j.foodchem.2022.133406
13. T. Kocadağlı, V. Gökmen, Formation of acrylamide in coffee. Curr. Opin. Food Sci. **45**, 100842 (2022). https://doi.org/10.1016/j.cofs.2022.100842
14. R. Monsalve-Atencio, D. Montaño-Montoya, J. Contreras-Calderón, (2025) Towards the Industrial Application of Ionic Liquids as Green and Smart Extraction Media in the Food and Wastewater Field. In: Vega-Castro OA, Simpson R, Pilar Buera M del, et al (eds) Selected Topics in Food Process Engineering. Springer Nature Switzerland, Cham, pp 255–292
15. R. Monsalve-Atencio, D.F. Montaño, J. Contreras-Calderón, Molecular imprinting technology and poly (ionic liquid)s: Promising tools with industrial application for the removal of acrylamide and furanic compounds from coffee and other foods. Crit. Rev. Food Sci. Nutr. **63**, 6820–6839 (2023). https://doi.org/10.1080/10408398.2022.2038078
16. R. Monsalve-Atencio, J. Contreras-Calderón, L.F. Giraldo, Synthesis of novel molecularly imprinted polymers based on ionic liquids with a biocompatible approach for acrylamide removal. Eur. Polym. J. **236**, 114075 (2025). https://doi.org/10.1016/j.eurpolymj.2025.114075
17. L. Guo, Q. Deng, G. Fang et al., Preparation and evaluation of molecularly imprinted ionic liquids polymer as sorbent for online solid-phase extraction of chlorsulfuron in environmental water samples. J. Chromatogr. A **1218**, 6271–6277 (2011). https://doi.org/10.1016/j.chroma.2011.07.016
18. R. Monsalve-Atencio, D. Montaño-Montoya, J. Contreras-Calderón, Molecularly Imprinted Polymers: An Emerging Strategy with Potential for Industrial-Scale Extraction in the Food and Wastewater Field, in *Selected Topics in Food Process Engineering*, ed. by O.A. Vega-Castro, R. Simpson, del M. Pilar Buera et al. (Springer Nature Switzerland, Cham, 2025), pp. 207–253
19. S. Ding, Z. Lyu, X. Niu et al., Integrating ionic liquids with molecular imprinting technology for biorecognition and biosensing: A review. Biosens. Bioelectron. Biosens. Bioelectron. **149**, 111830 (2020). https://doi.org/10.1016/j.bios.2019.111830
20. H. Liu, P. Jin, F. Zhu et al., A review on the use of ionic liquids in preparation of molecularly imprinted polymers for applications in solid-phase extraction. TRAC Trends Anal. Chem. **134**, 116132 (2021). https://doi.org/10.1016/j.trac.2020.116132
21. A.R. Bagheri, M. Arabi, M. Ghaedi et al., Dummy molecularly imprinted polymers based on a green synthesis strategy for magnetic solid-phase extraction of acrylamide in food samples. Talanta. **195**, 390–400 (2019)
22. M. Moeenfard, L. Rocha, A. Alves, Quantification of Caffeoylquinic Acids in Coffee Brews by HPLC-DAD. J. Anal. Methods Chem. **2014**, 965353 (2014). https://doi.org/10.1155/2014/965353
23. A. Santanatoglia, S. Angeloni, D. Bartolucci et al., Effect of brewing methods on acrylamide content and antioxidant activity: Studying eight different filter coffee preparations. Antioxidants. **12**, 1888 (2023)
24. R. Monsalve-Atencio, J. Contreras-Calderón, C.A. Pérez, L.F. Giraldo, Extraction of 5-(Hydroxymethyl)furfural using Molecular Imprinting Polymers Based on Ionic Liquids Derived from Organic Acids. ACS Appl. Polym. Mater. **8**, 5397–5409 (2026). https://doi.org/10.1021/acsapm.5c04057
25. E. Bacalum, M. Cheregi, V. David, Retention behaviour of some benzodiazepines in solid-phase extraction using modified silica adsorbents having various hydrophobicities. Rev. Roum Chim. **60**, 891–898 (2015)
26. S. Chigome, N. Torto, Electrospun nanofiber-based solid-phase extraction. TRAC Trends Anal. Chem. **38**, 21–31 (2012). https://doi.org/10.1016/j.trac.2012.04.011
27. E. Bacalum, A. Tanase, V. David, Retention mechanisms applied in solid phase extraction for some polar compounds. Univ. Bucar Chim. **19**, 61–68 (2010)
28. A. Gossard, L. Henriet, S. Vannier et al., Emulsion synthetic route of hierarchically porous zeolite-geopolymer composites for Sr2 + decontamination in fixed bed process. Ceram. Int. **50**, 19692–19701 (2024). https://doi.org/10.1016/j.ceramint.2024.03.090
29. K.F. Handle, R. Bakry, G.K. Bonn, Phosphonium based anion exchange resin for enrichment of phenolic acids. J. Chromatogr. A **1700**, 464049 (2023). https://doi.org/10.1016/j.chroma.2023.464049
30. E. Bacalum, M. Radulescu, E.-E. Iorgulescu, V. David, Breakthrough parameters of SPE procedure on C18 cartridges for some polar compounds. Rev. Roum Chim. **56**, 137–143 (2011)
31. A. Grandjean, Y. Barré, A. Hertz et al., Comparing hexacyanoferrate loaded onto silica, silicotitanate and chabazite sorbents for Cs extraction with a continuous-flow fixed-bed setup: Methods and pitfalls. Process Saf. Environ. Prot. **134**, 371–380 (2020). https://doi.org/10.1016/j.psep.2019.12.024
32. M. Mesías, F.J. Morales, Acrylamide in coffee: Estimation of exposure from vending machines. J. Food Compos. Anal. **48**, 8–12 (2016). https://doi.org/10.1016/j.jfca.2016.02.005
33. F.L. Moreno, M. Raventós, E. Hernández et al., Rheological Behaviour, Freezing Curve, and Density of Coffee Solutions at Temperatures Close to Freezing. Int. J. Food Prop. **18**, 426–438 (2015). https://doi.org/10.1080/10942912.2013.833221
34. R. Monsalve-Atencio, K. Sanchez, J. Camaño et al., (2021) Determination of ochratoxin a in coffee by ELISA method and its relationship with the physical, physicochemical and microbiological properties. Vitae 28:. https://doi.org/10.17533/udea.vitae.v28n2a343838
35. F. Gómez-Narváez, M. Mesías, C. Delgado-Andrade et al., Occurrence of acrylamide and other heat-induced compounds in panela: Relationship with physicochemical and antioxidant parameters.

Food Chem. **301**, 125256 (2019). https://doi.org/10.1016/j.foodchem.2019.125256
36. D.H.H. Nguyen, A. Muthu, H. El-Ramady et al., Detection and formation of fluorescent carbon nanodots in coffee brews and its relationship with other compositions. J. Food Compos. Anal. **132**, 106347 (2024). https://doi.org/10.1016/j.jfca.2024.106347
37. N. Surapong, R. Burakham, Magnetic Molecularly Imprinted Polymer for the Selective Enrichment of Glyphosate, Glufosinate, and Aminomethylphosphonic Acid Prior to High-Performance Liquid Chromatography. ACS Omega. **6**, 27007–27016 (2021). https://doi.org/10.1021/acsomega.1c03488
38. K. Bielicka-Daszkiewicz, A. Voelkel, Theoretical and experimental methods of determination of the breakthrough volume of SPE sorbents. Talanta. **80**, 614–621 (2009). https://doi.org/10.1016/j.talanta.2009.07.037
39. W. Wei, J. Li, X. Qi et al., Synthesis and characterization of a multi-sensitive polysaccharide hydrogel for drug delivery. Carbohydr. Polym. **177**, 275–283 (2017). https://doi.org/10.1016/j.carbpol.2017.08.133
40. H.M. Awad, R. Diaz, R.A. Malek et al., Efficient Production Process for Food Grade Acetic Acid by Acetobacter aceti in Shake Flask and in Bioreactor Cultures. J. Chem. **9**, 965432 (2012). https://doi.org/10.1155/2012/965432
41. H.Z. Şenyuva, V. Gökmen, Study of acrylamide in coffee using an improved liquid chromatography mass spectrometry method: Investigation of colour changes and acrylamide formation in coffee during roasting. Food Addit. Contam. **22**, 214–220 (2005). https://doi.org/10.1080/02652030500109834
42. van G. Wissen, J.W. Lowdon, T.J. Cleij et al., Porogenic solvents in molecularly imprinted polymer synthesis: A comprehensive review of current practices and emerging trends. Polym. (Basel). **17**, 1057 (2025)
43. F. Meier, B. Schott, D. Riedel, B. Mizaikoff, Computational and experimental study on the influence of the porogen on the selectivity of 4-nitrophenol molecularly imprinted polymers. Anal. Chim. Acta. **744**, 68–74 (2012). https://doi.org/10.1016/j.aca.2012.07.020
44. N. Cordoba, M. Fernandez-Alduenda, F.L. Moreno, Y. Ruiz, Coffee extraction: A review of parameters and their influence on the physicochemical characteristics and flavour of coffee brews. Trends Food Sci. Technol. **96**, 45–60 (2020). https://doi.org/10.1016/j.tifs.2019.12.004
45. G.A. Burlingame, A.M. Dietrich, A.J. Whelton, Understanding the basics of tap water taste. J. AWWA **99**, 100–111 (2007). https://doi.org/https://doi https://doi.org/10.1002/j.1551-8833.2007.tb07930.x
46. M. Charles-Bernard, K. Kraehenbuehl, A. Rytz, D.D. Roberts, Interactions between Volatile and Nonvolatile Coffee Components. 1. Screening of Nonvolatile Components. J. Agric. Food Chem. **53**, 4417–4425 (2005). https://doi.org/10.1021/jf048021q
47. E.K. Bekedam, M.J. Loots, H.A. Schols et al., Roasting Effects on Formation Mechanisms of Coffee Brew Melanoidins. J. Agric. Food Chem. **56**, 7138–7145 (2008). https://doi.org/10.1021/jf800999a
48. D. Gniechwitz, N. Reichardt, E. Meiss et al., Characterization and Fermentability of an Ethanol Soluble High Molecular Weight Coffee Fraction. J. Agric. Food Chem. **56**, 5960–5969 (2008). https://doi.org/10.1021/jf800231q
49. M.F. Kurniawan, N. Andarwulan, N. Wulandari, M. Rafi, Metabolomic approach for understanding phenolic compounds and melanoidin roles on antioxidant activity of Indonesia robusta and arabica coffee extracts. Food Sci. Biotechnol. **26**, 1475–1480 (2017). https://doi.org/10.1007/s10068-017-0228-6
50. I. Andriot, J.-L. Le Quéré, E. Guichard, Interactions between coffee melanoidins and flavour compounds: impact of freeze-drying (method and time) and roasting degree of coffee on melanoidins retention capacity. Food Chem. **85**, 289–294 (2004). https://doi.org/10.1016/j.foodchem.2003.07.007
51. T. Hofmann, M. Czerny, S. Calligaris, P. Schieberle, Model Studies on the Influence of Coffee Melanoidins on Flavor Volatiles of Coffee Beverages. J. Agric. Food Chem. **49**, 2382–2386 (2001). https://doi.org/10.1021/jf0012042
52. S. Pastoriza, J. Rufián-Henares, F.J. Morales, Reactivity of acrylamide with coffee melanoidins in model systems. LWT - Food Sci. Technol. **45**, 198–203 (2012). https://doi.org/10.1016/j.lwt.2011.08.004
53. G.D.T.M. Jayasinghe, A. Moreda-Piñeiro, Molecularly imprinted polymers for dispersive (micro) solid phase extraction: A review. Separations. **8**, 99 (2021)
54. M. Moeenfard, J.A. Silva, N. Borges et al., Diterpenes in espresso coffee: impact of preparation parameters. Eur. Food Res. Technol. **240**, 763–773 (2015). https://doi.org/10.1007/s00217-014-2381-y
55. I. López-Galilea, De M.P. Peña, C. Cid, Correlation of Selected Constituents with the Total Antioxidant Capacity of Coffee Beverages: Influence of the Brewing Procedure. J. Agric. Food Chem. **55**, 6110–6117 (2007). https://doi.org/10.1021/jf070779x
56. P.A.M. Barriga, R.Y.R. Pardo, F.L.M. Moreno, *Effect of extraction processing parameters using a* (ribbon blender on the physicochemical properties of coffee, 2024)
57. M. Geethalaxmi, C.K. Sunil, A. Rawson, N. Venkatachalapathy, Tamarind seeds: Potential valorisation as coffee substitute-roasting and its characterization. Food Humanity. **4**, 100563 (2025). https://doi.org/10.1016/j.foohum.2025.100563
58. E. Porto, E.G. Alves Filho, L.M.A. Silva et al., Ozone and plasma processing effect on green coconut water. Food Res. Int. **131**, 109000 (2020). https://doi.org/10.1016/j.foodres.2020.109000
59. B. Yuan, M.-G.C. Danao, J.E. Stratton et al., High pressure processing (HPP) of aronia berry purée: Effects on physicochemical properties, microbial counts, bioactive compounds, and antioxidant capacities. Innovative Food Sci. Emerg. Technol. **47**, 249–255 (2018). https://doi.org/10.1016/j.ifset.2018.03.009
60. F.J. Morales, Application of capillary zone electrophoresis to the study of food and food-model melanoidins. Food Chem. **76**, 363–369 (2002). https://doi.org/10.1016/S0308-8146(01)00295-3
61. T. Viencz, L.B. Acre, R.B. Rocha et al., Caffeine, trigonelline, chlorogenic acids, melanoidins, and diterpenes contents of Coffea canephora coffees produced in the Amazon. J. Food Compos. Anal. **117**, 105140 (2023). https://doi.org/10.1016/j.jfca.2023.105140
62. J. Contreras-Calderón, D. Mejía-Díaz, M. Martínez-Castaño et al., Evaluation of antioxidant capacity in coffees marketed in Colombia: Relationship with the extent of non-enzymatic browning. Food Chem. **209**, 162–170 (2016). https://doi.org/10.1016/j.foodchem.2016.04.038
63. F.M. Mehaya, A.A. Mohammad, (2020) Thermostability of bioactive compounds during roasting process of coffee beans. Heliyon 6:. https://doi.org/10.1016/j.heliyon.2020.e05508
64. N.Z. Rao, M. Fuller, Acidity and Antioxidant Activity of Cold Brew Coffee. Sci. Rep. **8**, 16030 (2018). https://doi.org/10.1038/s41598-018-34392-w
65. A. Vega, S.M. Reyes, J. Troestch, Physicochemical Parameters and Multivariate Analysis to Predict the Sensory Quality in Specialty Coffee from Panama. ACS Omega. **10**, 13251–13259 (2025). https://doi.org/10.1021/acsomega.4c10914
66. X. Wang, L.-T. Lim, Effects of grind size, temperature, and brewing ratio on immersion cold brewed and French press hot brewed coffees. Appl. Food Res. **3**, 100334 (2023). https://doi.org/10.1016/j.afres.2023.100334